Chaos in a Coulombic muffin-tin potential

S.Brandis
II. Institut für Theoretische Physik, Luruper Chaussee 149, 22761 Hamburg, Germany
(Received 17 November 1994)

We study the two-dimensional classical scattering dynamics by a muffin-tin potential with three Coulomb singularities. A complete symbolic dynamics for the periodic orbits is derived. The classical periodic trajectories are shown to be hyperbolic everywhere in phase space and to carry no conjugate points. We further determine all quantities that are characteristic for a chaotic system by the concept of the topological pressure.

PACS number(s): 05.45.+b, 34.80.−i, 72.10.−d

I. INTRODUCTION

In recent years the study of chaotic dynamical systems has attracted a lot of attention [1]. However, there are only a few models for which the dynamics is known to be completely chaotic. Well defined properties like ergodicity or complete hyperbolicity of the dynamics in phase space is usually very hard to prove. Systems for which a proof has been found are usually either Euclidean billiards with nontrivial boundaries or motion on Riemann surfaces endowed with a hyperbolic metric [1]. In contrast, for potentials there are hardly any examples for which these properties can be shown rigorously.

A few years ago an outstanding work by Knauf and Klein [2] gave an example of ergodicity in a potential problem using rather sophisticated mathematical tools. It treats the classical two-dimensional scattering by a rather general potential, whose main features are n fixed attractive Coulomb centers and a fast decay towards infinity. For $n \geq 3$ the system exhibits all the typical characteristics of chaotic scattering. On the set of bounded orbits the motion is proven to be ergodic (with respect to a specified measure).

However, some open problems remain, of which we would like to pick out the following two. For one, nobody has actually calculated periodic orbits beyond the proof of their existence as it turns out to be rather difficult. The periodic orbits yield a lot more insight into the detailed properties of the classical system. Moreover, there seems to be no path in sight to treat the quantum mechanical problem in the general setting given by Knauf and Klein, e.g., an exact way to determine resonances.

We study here a slightly different model in order to discuss the two above mentioned open questions. The classical part is the content of this paper. We derive a different, much simpler symbolic dynamics at the price of giving up the smoothness and generality of the potential. The quantum mechanical treatment as well as the semiclassical analysis will be the subject of a forthcoming presentation [3].

A similar model is discussed also by Gutzwiller in Chapter 20 of his book [1]. Again, no explicit results are known. In particular, the symbolic representation is different from ours, because we concentrate on periodic orbits rather than scattering orbits which are the subject in [1].

The paper is organized as follows. In Sec. II we discuss the main features of the model. We show a way to find periodic orbits in Sec. III. Moreover, we calculate all periodic orbits up to code length $N = 17$ and discuss some of their statistical properties. These are, e.g., the topological entropy, the distribution around a code length, and the nearest neighbor spacing. Section IV is devoted to stability properties of periodic orbits. We present a way to determine them for any given potential and will specify it for our case by actual calculation. The mean Lyapunov exponent and its spread around this value are a subject of our study as well. In Sec. V we use the topological pressure, known in the context of the thermodynamic formalism [4], to calculate various quantities characterizing the chaotic dynamics. All quantities are determined at different energies, since this is not a scaling parameter of the potential. We shall finish with some concluding remarks and an outlook on the quantum mechanical problem.

II. THE MODEL

The two-dimensional Hamiltonian system we consider is a potential scattering process. One particle scatters on a locally fixed potential which is defined in the following way:

$$V(\vec{r}) = \begin{cases} -\sum_{i=1}^{3} \left(\frac{Z_i}{|\vec{r} - \vec{s}_i|} - \frac{Z_i}{R_i} \right) & \text{for} \quad |\vec{r} - \vec{s}_i| \leq R_i \\ 0 & \text{else} . \end{cases} \tag{1}$$

These are three distinct fixed Coulomb potentials located on points $\vec{s}_i$ in configuration space, each being cut off beyond a radius $R_i, i = 1, 2, 3$. They do not overlap. The strength Z_i of each of the singularities is chosen to be positive, such that the potential is purely attractive. The constant terms $\frac{Z_i}{R_i}$ added to each site lift the potential as a whole and make it continuous. In a continuous potential, the momentum of the moving particle is continuous

and thus the trajectory is a once differentiable curve in configuration space. This is a typical muffin-tin (MT) potential indicated by the dotted lines in Fig. 1. As we shall be concerned with scattering, the energy is always positive, $E > 0$. One can imagine this being an idealized molecule, where an electron scatters off the protons. In the calculation we have chosen values for the constants such that the energy scale in the figures is of the order of eV.

Studying the solutions of the Hamiltonian system is equivalent to studying the geodesic motion on a surface with a metric defined via $(i, j = 1, 2)$

$$g_{ij}^{E}(\vec{r}) := \left(1 - \frac{V(\vec{r})}{E}\right) \delta_{ij}, \tag{2}$$

changing the time to arc length [5]. The superscript expresses the explicit energy dependence of the solutions, which is a decisive difference from billiards, where the action scales with the energy. The metric is not well defined at the Coulomb centers $\vec{s}_i$ as it is infinite there, but the time a trajectory needs to hit the center is finite. The most natural thing is thus to "regularize" these points and to extend the geodesic flow to the singularities by adding a backscattering orbit whenever there is a collision with a center. By this construction one can use important results of differential geometry, e.g., we can calculate the Gaussian curvature for this metric. It vanishes outside a MT and is strictly negative within,

$$K^{E}(\vec{r}) = -\frac{Z_i}{2E - \frac{Z_i}{R_i}\left(|\vec{r} - \vec{s}_i| + \frac{Z_i}{E - \frac{Z_i}{R_i}}\right)^3}. \tag{3}$$

This is a crucial property for the chaotic behavior as we shall see later. Note that its limit, when approaching a singularity, is finite.

The traditional way of studying scattering is to look at quantities like the cross section or the time-delay function. A characteristic of irregular scattering is the self-similar structure of singularities in these quantities [6]. These are consequences of the existence of a dense set of hyperbolic periodic orbits in phase space, which are therefore sometimes called the "skeleton" of phase space. As they determine the main structure, we will directly draw attention to these periodic geodesics instead of the scattering orbits. The meaning of these orbits will become clear in Sec. V in particular.

III. PERIODIC ORBITS

To find all periodic orbits systematically one usually needs to have a symbolic dynamics. This provides a well

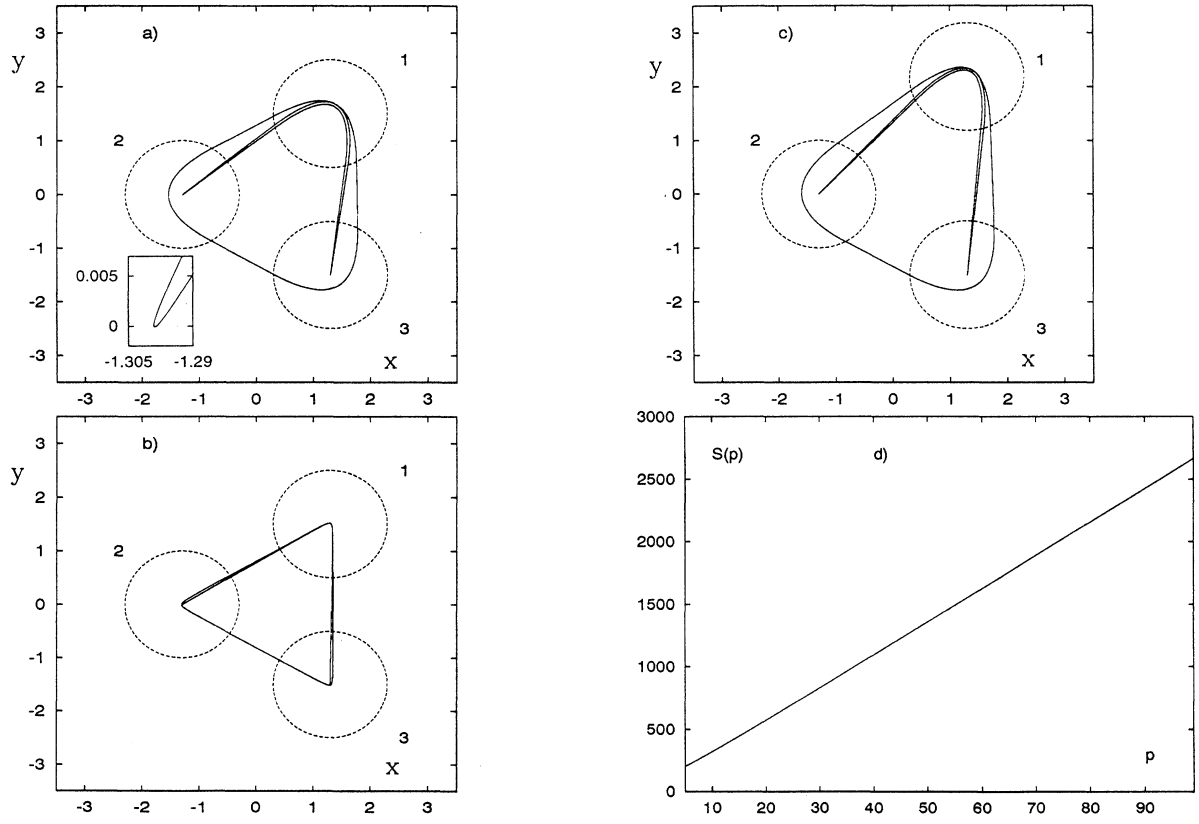

FIG. 1. The periodic orbit corresponding to the code word (1231213) for an equilateral configuration of MT's with (a) $E = 8$ and (b) $E = 50$. The inset in (a) is an enlargement of nucleus number 2 to show that the orbit does not collide. (c) shows the same orbit in a slightly asymmetric setting ($E = 50$). The dashed lines encircle the regions of nonvanishing potential. In (d) one can see how the action of this orbit changes with p, where $p^2 = 2E$.

defined enumeration and a check for completeness. We shall first present the code by which the periodic orbits (PO's) can be represented in a symbolic way. Then we describe the algorithm that finds the exact positions of the PO's in phase space.

There are two restrictions to the method applied below. (1) The code is valid for energies $E > \max(\frac{Z_i}{R_i})$ only. This is due to the fact that it requires the Kepler trajectories to be hyperbolas. (2) The centers $\vec{s}_i$ have to be arranged on the corners of a (convex) triangle, such that the corridors on which trajectories can move between two MT's do not intersect. Examples are given below (see Fig. 1). There are indications that this code can readily be generalized to more than three centers as long as they are placed on the corners of a convex polygon.

The code is in fact fairly simple. Giving each center a number (1,2,3) a periodic orbit is uniquely represented by its history in terms of the centers it passes during one traversal. That is to say, all periodic sequences in the space of words of the letters $(1,2,3)$, without repetition and modulo cyclic permutation, represent symbolically the set of all periodic orbits. When the Kepler trajectories are hyperbolas, a repetition of equal numbers cannot occur, because an orbit has to touch another MT before turning around the first one a second time. We shall now show this one-to-one relation.

(i) For an orbit to be periodic, it has to turn around the centers again and again. Hence, given a periodic orbit, it has a well defined path through the MT's and thus a single code (modulo its cyclic permutations).

(ii) Given a code one needs to show that there is only one PO. We shall exclude for a moment the orbits colliding with a singularity. Since the points $\vec{s}_i$ are then excluded, two orbits cannot be transformed continuously into each other, i.e., they are not homotopic, when they turn around the same center in a different orientation at least once during their traversal of the orbit. As the code is fixed, we know which centers the PO passes during the traversal. Any other orbit with this code is either (a) homotopic to the first one or (b) topologically different, which means that it runs around one of the MT's in a different orientation.

We can already exclude (a), since we know that the Gaussian curvature is nonpositive, which allows only one geodesic per homotopy class (see, e.g., [13]). To exclude (b) we split up the code into smaller parts and find three different types of pieces a periodic code can consist of.

(1) *...abc...*, where $a,b,c \in \{1,2,3\}$ and $a \neq c$. Whether the orbit turns around b clockwise or anticlockwise (see Fig. 1) is fixed by the explicit numbers, because the Kepler orbit being a hyperbola does not allow self-crossing after one turn. Hence given a sequence like the one above in a code the orbit has a well defined orientation.

(2) *...cabab...ababc...* in the familiar notation. On the pendulumlike motion between a and b the scattering angle spreads or decreases constantly because of the hyperbolas at each center. Thus it will not change the orientation in between, when it comes out the same way it went in. This is the case in (2), since the last three letters are just a cyclic permutation of the first three.

(3) *...cabab...abac...* . In this case the orientation has to change, as it comes out of the pendular motion the opposite way it went in. But as a result of the avoided self-crossing the turn around will happen exactly in the middle of the term. The pattern looks like a squeezed ancient Greek meander.

Finally, the orbits colliding with a center have to have a mirror symmetry in their code because of their backscattering nature. In fact, every code with this symmetry is a colliding one, which is then unique.

Given a one-to-one code with an appealing geometrical interpretation, we can construct each periodic orbit by an algorithm. The PO consists of pieces of free motion and Kepler trajectories. Passing the MT with number i in the code word, the orbit sweeps over an angle given by a Kepler hyperbola. The scattering angle therefore is given by conversion of the famous parametrization of a Kepler trajectory [thus the index in Eq. (4)] plus an additional piece coming from the impact parameter $\frac{l_i}{p}$, when it hits the boundary:

$$(\theta_{i+1}-\theta_i)_{\text{Kep}} = \operatorname{sgn}(l_i)\left\{2\arccos\left[\left(\frac{P_i}{R_i}-1\right)\frac{1}{\varepsilon_i}\right]-\pi\right\} + \arcsin\left(\frac{l_i}{pR_i}\right). \tag{4}$$

It is a function of the incoming relative angular momentum l_i. Here θ_i is the direction of the momentum before the ith center and P_i and ε_i are the parameters of the Kepler trajectory $\left(P_i=\frac{l_i^2}{Z_i}, \varepsilon_i^2 = 1+\frac{2(E-\frac{Z_i}{R_i})l_i^2}{Z_i^2}\right)$. In all calculations we have set the mass to 1. Note in the definition of the parameter ε_i that the energy is reduced here by $\frac{Z_i}{R_i}$ as a consequence of lifting the potential in the beginning. p is the absolute value of the momentum of the free motion.

On the other hand, the relative angular momenta (relative to the appropriate MT) transform into each other by geometrical arguments

$$l_{i+1} = l_i + |\vec{s}_i - \vec{s}_{i+1}|\, p\, \sin(\alpha_{i,i+1}-\theta_{i+1}), \tag{5}$$

$\alpha_{i,i+1}$ being the angle of the vector $\vec{s}_i - \vec{s}_{i+1}$ with respect to the x axis in a Cartesian coordinate system (see Fig. 1). Taking the inverse, we arrive at an additional, purely geometrical condition for two consecutive scattering angles as a function of the angular momentum

$$(\theta_{i+1}-\theta_i)_{\text{geo}} = \alpha_{i,i+1}-\alpha_{i-1,i} - \left[\arcsin\left(\frac{l_{i+1}-l_i}{|\vec{s}_i-\vec{s}_{i+1}|\,p}\right) - \arcsin\left(\frac{l_i-l_{i-1}}{|\vec{s}_{i-1}-\vec{s}_i|\,p}\right)\right]. \tag{6}$$

For periodic orbits (and for each index i) the functions in (4) and (6) have to be equal. Thus the problem of determining PO's is reduced to finding the zeros of the difference of (4) and (6) in N-dimensional angular space as a function on the N-dimensional angular momentum space, when the length of the code is N.

In general, the problem of finding a root in an N-dimensional system of transcendental equations can be

rather difficult numerically, depending on the explicit function. In this case, however, we find that it works very well. We only have to keep track of the variables l_i staying in their domain and give a good first guess for the root. The latter can easily be constructed by the code. This guarantees fast convergence. But even for starting values far away from the solution, we always find a single solution, as it should be from the above proof for the uniqueness of the code. As an intuitive argument one can imagine the good convergence coming from the monotonicity of the arc functions. We have tested this up to code length 17, which corresponds to 16 510 primitive orbits, i.e., orbits that are traversed only once. There are 107 more when one includes multiple traversals. $N = 17$ is not a limit of this method, but a practical (preliminary) one, as the CPU time increases exponentially with the code length. Figure 1 shows a typical orbit, this one belonging to the code word (1231213). In Figs. 1(a) and 1(b) the MT's are located on an equilateral triangle and only the energy is changed from $E = 8$ to $E = 50$, respectively. As the solutions do not scale with the energy, because the potential contains internal scales like the radius of each MT and the distances between them, the periodic orbits vary with the energy. However, the topologically different orbits become geometrically very similar as the energy rises. This gives rise to a number of nongeneric features in quantities we shall look at in the following. The effect of the high symmetry of the equilateral triangle on the classical dynamics has been studied intensively in the works on three disks [7]. Instead of reducing our system to the fundamental domain to extinguish the nongeneric symmetries, we vary the positions of the MT's. In Fig. 1(c) the angles of the triangle are slightly changed to be 50°, 60°, 70°, again representing the same orbit.

The number of periodic orbits $N(T)$ with periods below a certain period T proliferates exponentially in chaotic systems. The topological entropy τ determines the rate of increase. That is to say that asymptotically

$$N(T) \approx \frac{\exp(\tau T)}{\tau T} \quad \text{as } T \to \infty. \tag{7}$$

In our case this is strongly linked to the exponential increase of the number of code words. If $Z(N)$ denotes the number of all primitive periodic codes of length N, it is given by the recursion relation

$$Z(N) = \frac{1}{N}\left(2^N + (-1)^N 2 - \sum_{m|N} m\, Z(m)\right), \tag{8}$$

where the sum runs over all divisors m of N. To understand this formula, one starts by noticing that there are 2^N possibilities to create a code word (without repetitions) of length N out of three letters. Implementing the periodicity condition, subtracting all multiples of smaller code words, and dividing by the number of permutations N, one arrives at Eq. (8). Thus the number of code words increases exponentially with a rate of $\ln 2$ (sometimes this is also called topological entropy of the number of code words). At high energies the period becomes essentially a multiple of the free parts of the orbit as shown in Fig. 2. As one can see from Eq. (2) or (3) the metric becomes nearly flat as we go to very high energies. The pronounced staircase behavior washes out only as one gets to longer PO's, which is a difficult region to reach numerically, or to lower energies as in Fig. 2(b). To eliminate the nongeneric staircase we destroy the high symmetry by changing the equilateral triangle as above. The effect on $N(T)$ can be seen in Fig. 2(c).

To determine the topological entropy, we fit an exponential to the staircase function. As we only know the asymptotic behavior, there is a freedom in choosing the fitting function, as long as the asymptotic behavior remains the same. Experience with a lot of systems has shown that the exponential integral $\mathrm{Ei}(x)$ usually leads to a much better fit. It is defined as the principal value of $\int_x^\infty \frac{\exp t}{t}\, dt$. Figures 2(a)–2(c) confirm how well this function resembles the mean behavior, keeping in mind that we concentrate on the asymptotic behavior.

In the case of billiards one can define an energy independent entropy in units of the geometric length of the periodic orbits. Here there is no such simple *exact* relationship and we have to calculate it for each energy separately (see Table I). Nevertheless, in the high energy region, as the geometry of the orbits hardly changes any further, the classical action scales with $\sqrt{2E}$ approximately. As an example, Fig. 1(d) displays the energy dependence of the classical action of a typical orbit. This will have an effect especially in the semiclassical analysis [3].

Another interesting plot is the probability distribution $p_N(T)$ of periods for a given code length N. Thus we collect all orbits to a given code length N and determine the probability for different periods to appear. This has already been studied in the hyperbola billiard [8]. If one finds this distribution to approach a smooth Gaussian for large code length (and an overlap for different code lengths), there cannot be a minimal time ΔT of which all periodic orbits are just multiples. This in turn would prove a system [as long as it is an axiom A system (for a definition, see [9])] to be weakly mixing and to have the mentioned exponential asymptotic behavior of $N(T)$ [10,2]. Our numerical tests indicate this behavior (Fig. 2), although numerics in this context has to be viewed with much care. For one, the statistics is rather poor to overcome the strong geometric influence of the MT setting and we do not reach a Gaussian by far. Furthermore, the numerical spreading might as well be a consequence of larger multiples of a few basic lengths as has been pointed out by Knauf [11].

The nearest neighbor spacing (NNS) of energy levels in chaotic systems has been the subject of many discussions in the literature (see, e.g., [1]). By the semiclassical trace formula there is an interesting duality between the energy spectrum on the quantum mechanical side and the length spectrum of periodic orbits on the classical side. Thus it seems to be natural to ask whether the NNS statistics of the length spectrum reveals any characteristic features [8]. In our system we find the number of orbits to be not enough to give stable statistics. As one includes more and more orbits, it seems to approach a Poissonian rather than, e.g., a distribution of a spectrum

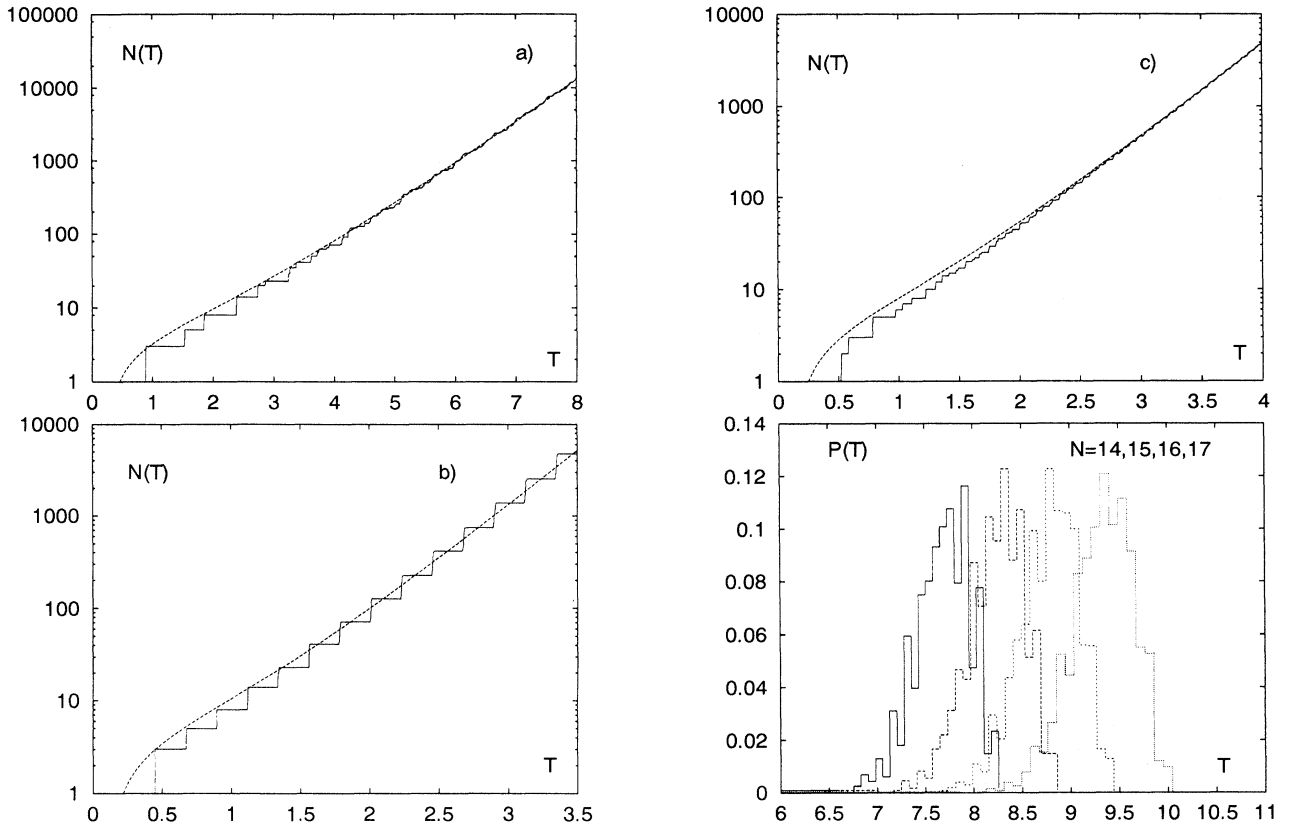

FIG. 2. $N(T)$ for the symmetric configuration at energies (a) $E = 10.125$ and (b) $E = 50$. The asymmetric case is shown in (c) ($E = 50$). The dashed lines show the fit to the function $\mathrm{Ei}(\tau T)$ for which the values of τ are given in Table I. (d) displays the distribution of lengths for code lengths 14, 15, 16, and 17 in the asymmetric system at energy 10.125 (full, dashed, dotted, and dashed-dotted, respectively).

due to an underlying ensemble of Gaussian orthogonal random matrices. This would agree with an observation made for other chaotic systems as well [8,12].

IV. STABILITY AND CONJUGATE POINTS

Given a periodic orbit or any other trajectory one can calculate its stability, i.e., the linear approximation of the motion in its vicinity. In practice one needs to find an orthogonal (local) coordinate system, which splits the motion into a direction parallel and a direction transversal to the flow. This is, in general, not a perfectly obvious procedure. In this case a particular problem comes about by the Coulomb singularities, such that the results obtained may easily be absurd, if one is not careful enough.

The most elegant way is to return to the geodesic motion generated by g_{ij}^E [2,13]. We know from differential geometry on two-dimensional surfaces that orthogonal coordinates always exist, called geodesic coordinates. The second variation of the Lagrangian on the surface leads to the Jacobi equation for the transversal component y of a vector field along the geodesic,

$$\ddot{y} + K^E(\vec{r}(s))\, y = 0, \tag{9}$$

with the Gaussian curvature in (3) given in terms of the arclength s in this metric. The dot denotes the derivative with respect to s. To calculate the stability in phase space we need to extend this to the 2×2 stability matrix $\mathbf{M}(s)$ which is obtained as a solution of

$$\dot{\mathbf{M}}_i(s) = \begin{pmatrix} 0 & 1 \\ -K_i^E & 0 \end{pmatrix} \mathbf{M}_i(s) \quad \text{with} \quad \mathbf{M}_i(0) = \begin{pmatrix} 1 & 0 \\ 0 & 1 \end{pmatrix}. \tag{10}$$

The index i labels the corresponding MT. By the negativity of the curvature, a solution of this equation is strictly positive, which is a manifestation of the hyperbolicity of the orbits. Note that a solution of a differential equation of this type has a constant determinant, which reflects

TABLE I. Values for τ and $\bar{\lambda}$ at various energies.

$p = \sqrt{2E}$	Config.	τ	$\bar{\lambda}$
4.5	sym.	1.48	2.19
	asym.	1.27	2.02
10	sym.	3.09	4.74
	asym.	2.69	4.28
30	sym.	8.72	12.47
	asym.	7.65	11.28

the Liouville theorem on the conservation of volume under the flow in phase space.

The stability matrix for a periodic orbit is often called the monodromy matrix. In our case it is a product of those matrices that correspond to the pieces the orbit traverses. The part for a free motion reads

$$\mathbf{M}_{\text{free}} = \begin{pmatrix} 1 & t_{\text{free}} \\ 0 & 1 \end{pmatrix}. \tag{11}$$

Here t_{free} is the time the orbit spends between two MT's. The eigenvalues of the monodromy matrix now determine the spreading of orbits. Since the determinant of the monodromy matrix is equal to 1, their eigenvalues are inverse to each other. As they are both positive, we can write them as exponentials and remain with the stability exponent as the only parameter, which is defined by

$$u(T) := \ln\left(\frac{1}{2}|\mathrm{Tr}\mathbf{M}(T)| + \sqrt{[\mathrm{Tr}\mathbf{M}(T)]^2 - 4}\right), \tag{12}$$

and

$$\lambda(T) := \frac{u(T)}{T} \tag{13}$$

determines the celebrated Lyapunov exponent. T is the period of the periodic orbit. These are strictly positive, because the solution of (10) is always positive and hence the orbits are hyperbolic.

The different features of energy dependence in the length spectrum manifest themselves in a similar manner in the Lyapunov or stability exponents. Figure 3(a) shows that the stability exponent becomes to a good approximation energy independent for large energies. It depends almost linearly on the period, where the spread around the mean widens as the energy decreases or the symmetry is destroyed [Fig. 3(b)]. Figure 3(c) displays the distribution of Lyapunov exponents around their mean in the most generic case, which is the asymmetric configuration at low energies. The arithmetical mean of the Lyapunov exponents $\bar{\lambda}_N$ is always larger than the topological entropy as can be seen in Table I, a typical feature for scattering systems. This plays an important role for the question of convergence of the semiclassical trace formula [14]. The index N states that we have taken the mean over all Lyapunov exponents up to code length N and $\bar{\lambda} := \lim_{N\to\infty} \bar{\lambda}_N$.

Not quite as vital for the classical discussion, but essential in the context of semiclassics, are the so called conjugate points. The number of conjugate points along a periodic orbit determines (if there are no further reflections on hard walls) the Maslov indices in the Gutzwiller trace formula [15].

Conjugate points can be understood in many ways. Further on we are going to sketch a proof for the fact that in this system there are no conjugate points along periodic orbits. For this purpose we present a picture of conjugate points that is closely linked to the reasoning of the proof. Imagine you are sitting on a trajectory in configuration space and start with various directions of the initial momenta. This fan of trajectories then spans a volume element in phase space. Whenever the dimension of this volume element shrinks on the trip through the trajectory, you have hit a point conjugate to your starting point. This is called a conjugate point. In some direction of phase space you have crossed a trajectory that has started at the same point, but in a different direction. Now we return to the more technical definition and demonstrate the absence of conjugate points in our MT model.

Let $c(s, v)$ be a geodesic parametrized by arclength s

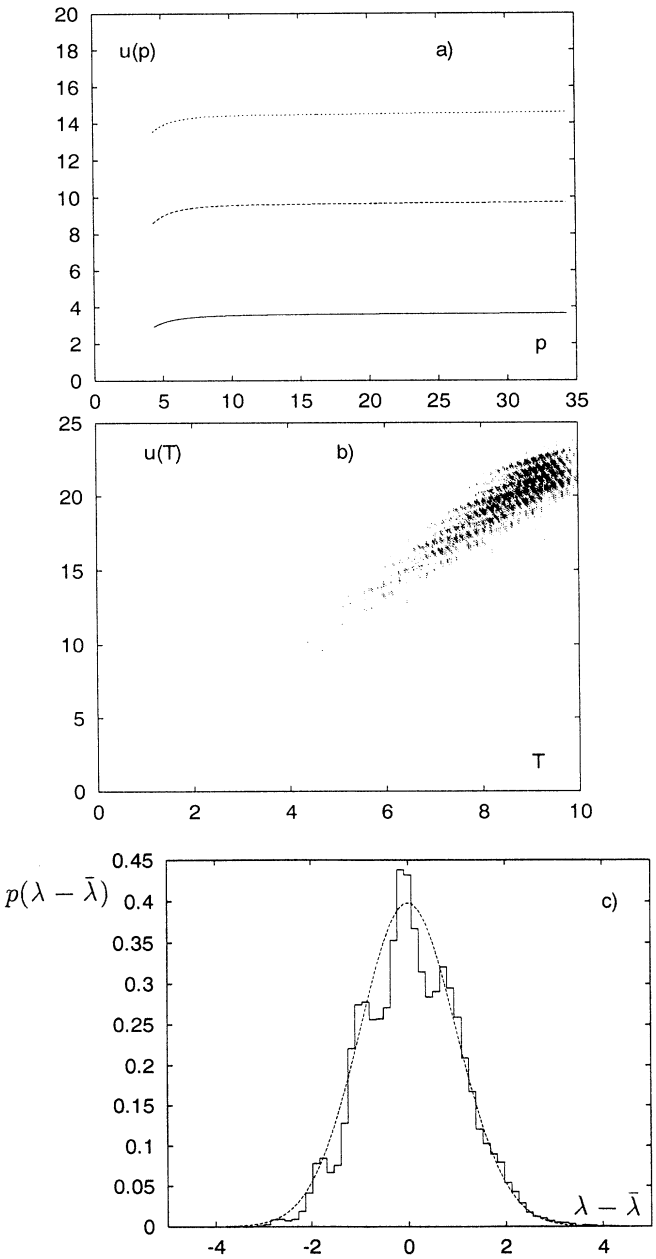

FIG. 3. Stability exponents (a) as a function of the momentum and (b) plotted against the period length (for $E = 10.125$ in the asymmetric case). (c) shows the distribution of Lyapunov exponents around their mean for the same setting.

and let v be a variation, such that for all values of v $c(s,v)$ is a geodesic. Running v spans a whole family of geodesics. A Jacobi field Y is a vector field along $c(s,v)$ generated by

$$Y(s) := \frac{\partial}{\partial v} c(s,v). \tag{14}$$

Taking geodesic coordinates and the dual basis in tangent space, one gets for the transversal component of the Jacobi field, let us call it $y(s)$, the Jacobi equation Eq. (9). As long as $c(s,v)$ is differentiable with respect to s, $y(s)$ is differentiable as well. Since the curvature $K^E \leq 0$, the solution of the Jacobi equation is either only convex or only concave [depending on the initial condition $\dot{y}(0)$]. But then it is impossible to find a nonvanishing, differentiable solution of the Jacobi equation with $y(0) = y(s_1) = 0\,, s_1 > 0$. So there are no conjugate points.

This is a slight extension of the proof found in [13] for nonsmooth $c(s,v)$. Note that $\dot{c}(s,v)$ has to be continuous.

V. TOPOLOGICAL PRESSURE

The central role of periodic orbits in dynamical systems — bounded as well as unbounded — becomes most obvious in the context of the thermodynamic formalism [4]. From this elaborate and abstract theory we shall only concentrate on a small part, namely, the concept of topological pressure $P(\beta)$. This enables us in principle to calculate various quantities that characterize a given chaotic system from the single function $P(\beta)$, such as topological entropy, mean Lyapunov exponents, escape rate, fractal dimensions, etc.

Starting with the *classical* time evolution operator (as compared to the more familiar quantum operator), one can define a Fredholm determinant that satisfies a secular equation for the determination of its eigenvalues [16]. The spectrum consisting of the fundamental modes of the system governs its dynamical evolution in time. Whereas for integrable systems the spectrum is found to be discrete, it is continuous for chaotic systems [9]. More detailed information about chaotic systems, though, is found in the structure of resonances found in complex mode space [16]. These will not be of interest to us here.

The above determinant can be expanded in terms of classical trajectories. It turns out that this leads to a product of so called ζ functions. The latter is a special case of the Ruelle zeta function $\zeta_\beta(s)$ [4]. In this particular case the factors in the infinite product over primitive periodic orbits are weighted by the stability. To be more precise, it is defined as

$$\zeta_\beta(s) = \prod_\gamma \{1 - \exp[-(s + \beta\lambda_\gamma)T_\gamma]\}^{-1}, \tag{15}$$

where γ labels the primitive periodic orbits, λ_γ denotes the Lyapunov exponent, and T_γ is the corresponding time of the periodic orbit. Its analyticity properties are well established. The zeta function $\zeta_\beta(s)$ is known to be analytic in the half-plane $\mathrm{Re}\, s > P(\beta)$ and has a pole at $\mathrm{Re}\, s = P(\beta)$. Thus it determines the abscissa of convergence of $\zeta_\beta(s)$, which means more accurately

$$P(\beta) := \inf\left\{\sigma \in \mathbb{R} | \sum_\gamma \exp[-(\sigma + \beta\lambda_\gamma)T_\gamma] < \infty\right\}. \tag{16}$$

The resonances all lie below this boundary. As the Euler product does not converge there, one needs different techniques for the analytical continuation to determine these poles.

Since we are only interested in $P(\beta)$, we simply have to find the highest root of $\zeta_\beta(s)^{-1}$, which we do by evaluation of Eq. (15). The result is plotted in Fig. 4. As λ and T are energy dependent, we show the result for various energies. The plots have been computed with the length spectrum of the asymmetric configuration. Numerically we have only a finite number of factors in (15), such that we can only approximate the root. We studied the quality of the behavior of the approximation as we include more and more orbits and finally extrapolate the root by fitting with a rational function. We have tested this procedure on the Riemann ζ function, where we know the result [the topological pressure is exactly $P(\beta) = 1 - \beta$] and achieve an accuracy of at least two decimals. An alternative method is to expand Eq. (15) into a Dirichlet series. This procedure is not as fast but allows much better accuracy (and gives consistent results) [16].

In Table II we have listed all quantities one can read off the topological pressure. In the following we shall explain them in more detail.

For $\beta = 0$ the Lyapunov exponents in Eq. (15) do not contribute and we are left with the lengths of the periodic orbits. The infinimum of real numbers σ that prevent the sum in Eq. (16) from divergence has to be just the growth rate of the number of prime periodic orbits. Thus we have $P(0) = \tau$, the topological entropy. Using this result, one can prove for $P(\beta)$ the more explicit form

$$P(\beta) = \tau - \beta\langle\lambda\rangle_\beta, \tag{17}$$

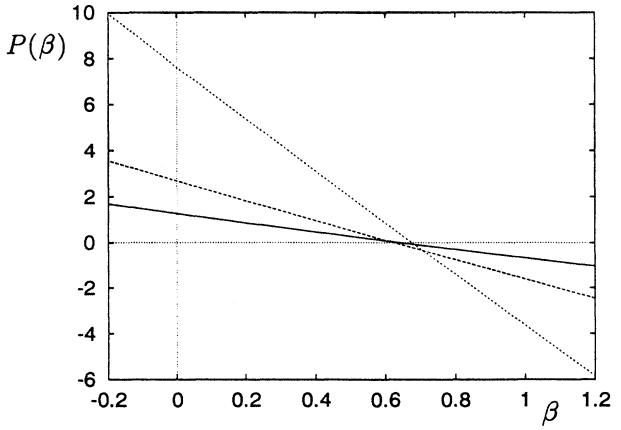

FIG. 4. The topological pressure at energies $E = 10.125$ (full), $E = 50$ (dashed), and $E = 450$ (dotted).

TABLE II. Dynamical quantities read off from the topological pressure in Fig. 4, corresponding to the asymmetric case.

$p =$	4.5	10	30
τ	1.27	2.69	7.60
$\bar{\lambda}$	2.02	4.30	11.32
Γ	0.64	1.62	3.65
$\hat{\lambda}$	1.81	4.29	11.18
h_{KS}	1.14	2.68	7.53
D_H	2.27	2.26	2.35
D_I	2.25	2.25	2.35

where the average $\langle\,\rangle_\beta$ is defined by

$$\langle\lambda\rangle_\beta := -\frac{1}{\beta}\lim_{T\to\infty}\frac{1}{T}\ln\left\{\frac{\sum_{T\le T_\gamma\le T+\delta}\exp\left(-\beta\lambda_\gamma T_\gamma\right)}{N(T+\delta)-N(T)}\right\} \tag{18}$$

and the limit is said to be independent of δ [17]. $N(T)$ is just the staircase function of Eq. (7). From this representation one can see after some calculation that $P'(0) = -\bar{\lambda}$. Thus we have determined τ and $\bar{\lambda}$ by two independent methods (cf. Secs. III and IV) and find very good agreement by comparing the values in Tables I and II.

A chaotic system produces information: Two initial conditions that are practically indistinguishable separate into two completely different states under the time evolution of the system. This is a consequence of the exponential divergence of two neighboring trajectories. A measure for this gain of information is the Kolmogorov-Sinai entropy h_{KS} (for an exact definition, see [18]). For a *bounded* system, it is linked to an average over Lyapunov exponents by $h_{\mathrm{KS}} = \hat{\lambda}$, where $\hat{\lambda} := -P'(1)$ [this average is more complicated than the arithmetical mean as one can see from the definition in Eq. (17)]. For an *unbounded* system, one has to take into account the number of orbits leaving the interaction region. They are "lost" for the growth of information. In chaotic systems the proportion of particles $n(T)$ that remain in the interaction region after the time T decays exponentially, i.e.,

$$n(T) \sim \exp\left(-\Gamma T\right), \tag{19}$$

and Γ is called the escape rate [7]. It is given here by $\Gamma := -P(1)$. In this case the Kolmogorov-Sinai entropy is determined by

$$h_{\mathrm{KS}} = \hat{\lambda} - \Gamma. \tag{20}$$

$P(\beta)$ is monotonic and convex in general [4]. This leads to inequalities of the form $\hat{\lambda} \le \bar{\lambda}$ and $h_{\mathrm{KS}} \le \tau$. In our case the topological pressure is nearly linear, a feature that has been observed for the three- and four-disk system as well, such that $\hat{\lambda} \approx \bar{\lambda}$ and $h_{\mathrm{KS}} \approx \tau$.

Another interesting and often discussed quantity is the fractal Hausdorff dimension D_H. It measures in a certain sense the fraction of phase space occupied by the strange repellor. We find it here via the root of the pressure, $P(d_H) = 0$, where $D_H = 2\,d_H + 1$. In bounded chaotic systems with two degrees of freedom, where the escape rate $\Gamma = 0$, such that $d_H = 1$, the repellor fills the whole phase space ($D_H = 3$). In our case the repellor is restricted to a fraction of the interaction region (see Table II). A similar measure is the information dimension $D_I = 2\,d_I + 1$, which is given by $d_I = \frac{h_{\mathrm{KS}}}{\hat{\lambda}}$. From the above inequalities we have $D_I \le D_H$ as is confirmed in Table II.

There is an obvious trend in the data of Table II from lower to higher energies. The topological entropy rises almost linearly with the momentum of the free particle. This is, however, somewhat misleading. The strong proliferation of orbits does not reflect that the system becomes "more chaotic." The increase in energy leads to shorter times of the periods, such that more orbits have accumulated below a fixed time T. Similarly, the escape rate reflects the fact that a particle escapes faster at higher energies. Somewhat surprising is the behavior of the Hausdorff dimension. There does not seem to be an overall trend, although intuitively one might expect the fractal dimension to shrink as the orbits tighten closer to the triangle of MT's. But as it is a measure in phase space, one needs to take into account the momentum dimension, which increases as the trajectories get closer to the centers of the MT's, where the momenta become large due to the Coulomb singularity.

VI. CONCLUSION

We have studied the classical scattering dynamics of a MT potential consisting of three Coulomb singularities. We find an exponential proliferation of hyperbolic periodic orbits using a complete symbolic dynamics. The rather old and well known analogy to differential geometry proves to be very handy in studying potential problems in general, especially for the calculation of the stability exponents. The geometry of the system has a large effect on the length spectrum in the limit of high energies. By calculating the topological pressure, we could determine all relevant quantities to characterize the classical motion.

Although the nonscaling behavior of the potential complicates the situation compared to a billiard at first sight, the completely defocusing nature of the potential facilitates it in other respects, e.g., all Lyapunov exponents are positive and there are no conjugate points. This will have an impact on the semiclassical discussion, which is our ultimate interest. The quantum mechanics and its semiclassical approximation will be the subject of the above mentioned forthcoming presentation [3].

I would like to thank Professor F. Steiner for many fruitful and encouraging discussions. This work was supported by Studienstiftung des deutschen Volkes.

[1] For example, M. C. Gutzwiller, *Chaos in Classical and Quantum Mechanics* (Springer, New York, 1990); *Chaos and Quantum Physics*, edited by M.-J. Giannoni, A. Voros, and J. Zinn-Justin (North-Holland, Amsterdam, 1991), and references therein.
[2] A. Knauf and M. Klein, *Classical Planar Scattering by Coulombic Potentials*, edited by W. Beigelböck, Lecture Notes in Physics Vol. 13 (Springer, Heidelberg, 1992).
[3] S. Brandis (unpublished).
[4] D. Ruelle, J. Stat. Phys. **44**, 281 (1986); *Thermodynamic Formalism* (Addison-Wesley, Reading, MA, 1978); P. Walters, *An Introduction to Ergodic Theory* (Springer, Berlin, 1981); see also articles in *Dynamical Systems II*, edited by Y. G. Sinai (Springer, Berlin, 1989).
[5] R. Abraham and J. E. Marsden, *Foundations of Classical Mechanics* (Benjamin, Reading, MA, 1978).
[6] For a recent review, see E. Ott and T. Tel, in Chaos **3**, 417 (1993).
[7] P. Gaspard and S. A. Rice, J. Chem. Phys **90**, 2225 (1989); **90**, 2242 (1989); **90**, 2255 (1989).
[8] M. Sieber and F. Steiner, Physica D **44**, 248 (1990).
[9] V. I. Arnold and A. Avez, *Ergodic Problems of Classical Mechanics* (Benjamin, New York, 1968).
[10] W. Parry and M. Pollicott, Ann. Math. **118**, 573 (1983).
[11] A. Knauf (private communication).
[12] M. Sieber, Ph.D. thesis, University of Hamburg, 1991 [DESY Report No. 91-030, 1991 (unpublished)].
[13] S. Gallot, D. Hulin, and J. Lafontaine, *Riemannian Geometry* (Springer, Berlin, 1990).
[14] R. Aurich, J. Bolte, C. Matthies, M. Sieber, and F. Steiner, Physica D **63**, 71 (1993).
[15] J. M. Robbins, Nonlinearity **4**, 343 (1991).
[16] P. Gaspard and D. Alonso Ramirez, Phys. Rev. A **45**, 8383 (1992).
[17] J. Bolte (private communication).
[18] J.-P. Eckmann and D. Ruelle, Rev. Mod. Phys. **57**, 617 (1985).